Theoretical and Applied Climatology (2025) 156:62
https://doi.org/10.1007/s00704-024-05252-7

RESEARCH

Multi-land-surface variables-precipitation coupling over the northeastern slope of the Tibetan Plateau

Zesu Yang[1] · Ping Yue[2] · Qiang Zhang[2] · Hang He[1] · Hongwei Yang[1]

Received: 23 May 2024 / Accepted: 7 November 2024 / Published online: 2 January 2025

Abstract
Land-atmosphere coupling is crucial for understanding the role of land surface conditions on precipitation, especially on the northeastern slope of the Tibetan Plateau, an area that has received limited attention. This study investigates the coupling between multiple land surface factors and precipitation, focusing on the individual and combined impacts of soil moisture, surface temperature, and vegetation (Leaf Area Index, LAI). The results reveal significant northwest-southeast gradients in surface factors, leading to corresponding spatial variations in latent (LE) and sensible heat fluxes (H). The two-stage land-atmosphere coupling were examined using complex correlation coefficients. In surface stage, the synergistic coupling of LE or H with soil moisture, surface temperature, and LAI is significantly enhanced compared to individual coupling. In atmosphere stage, after considering both surface fluxes and precipitation components, the coupling becomes notably stronger. Spatial differences in soil moisture and surface temperature mainly affect the surface factor-latent heat flux-precipitation coupling chain, while LAI impacts the surface factor-sensible heat flux-precipitation coupling chain. The synergistic coupling of surface variables with LE is strongest in forested areas, and with H in sparse vegetation areas, primarily driven by soil moisture. The synergetic coupling of LE and H with precipitation is relatively strong in forested and sparse vegetation areas, where precipitation is mainly dominated by H. These findings enhance our understanding of the comprehensive impact of multiple surface factors on precipitation under complex land surfaces and could provide scientific references for improving simulation of land-atmosphere coupling in weather and climate models.

1 Introduction

Land surface processes exert a significant influence on boundary layer development through the exchange of moisture and energy, orchestrating complex feedback mechanisms that finely regulate both temperature and precipitation patterns (Betts et al. 1996; Findell and Eltahir 1997). Spatial gradients in soil moisture could trigger mesoscale circulation and generate ascending motion in drier regions, leading to afternoon precipitation tending to occur in areas with drier soil moisture (Guillod et al. 2015; Petrova et al. 2018). Soil moisture also impacts near-surface air temperatures by regulating the distribution of surface energy. Drier regions and periods often result in the generation of heatwaves (Meng and Shen 2014; Seneviratne et al. 2006). Therefore, land-atmosphere interactions are a vital component of weather and climate research. Changes in land surface variables are important signals for seasonal and sub-seasonal forecasting, playing a crucial role in improving atmospheric predictability.

The enhancement of atmospheric predictability through land surface conditions exhibits considerable regional disparities, with significant impacts on atmospheric processes only occurring in regions characterized by strong land-atmosphere coupling. Assessing the extent to which changes in land surface conditions influence the response of atmospheric states or processes and investigating the spatiotemporal characteristics and mechanisms of land-atmosphere coupling can deepen our understanding of the role of the land surface in atmospheric predictability and climate change. Both observational and modeling studies

✉ Ping Yue
jqyueping@126.com

[1] School of Atmospheric Sciences, Plateau Atmosphere and Environment Key Laboratory of Sichuan Province, Chengdu University of Information Technology, Chengdu 610225, China

[2] Institute of Arid Meteorology, CMA, Key laboratory of Arid Climatic Change and Reducing Disaster of Gansu Province, Key Open Laboratory of Arid Climatic Change and Disaster Reduction of CMA, Lanzhou 730020, China

have indicated that regions with strong land-atmosphere coupling are typically situated in transitional zones between arid and humid climates (Koster 2004; Zeng et al. 2010). In these areas, atmospheric variables and surface fluxes are particularly sensitive to changes in land surface conditions, highlighting the significant contribution of the land surface to variations in atmospheric states.

Focusing on the spatiotemporal variations of land-atmosphere coupling and its influencing factors, extensive researches have been conducted in hotspots of land-atmosphere coupling. Soil moisture, with its memory of 1–2 months (Entin et al. 2000), is recognized as a crucial factor in enhancing seasonal predictions (Koster et al. 2004). Thus, present investigations predominantly concentrate on studying the coupling between soil moisture and atmospheric processes, as well as the impact of soil moisture on the spatial distribution of coupling (Li et al. 2017; Santanello et al. 2018). In terms of temporal dynamics, periods of higher moisture in arid regions and drier periods in humid regions tend to demonstrate stronger coupling (Gao et al. 2018; Ruscica et al. 2015; Wei and Dirmeyer 2012). This is because that the sensitivity of evapotranspiration to soil moisture is most notable in transitional climatic zones (Wei and Dirmeyer 2012). In contrast, in arid and humid regions surface evapotranspiration is insensitive to soil moisture due to too small evapotranspiration in arid region and energy controlling of evapotranspiration in humid region. Furthermore, analyses utilizing CMIP5 data reveal that under scenarios of low to moderate emissions, warming will intensify soil moisture-precipitation coupling in transitional climatic zones due to increased surface aridification (Dirmeyer et al. 2014; Zeng and Xie 2015).

Research has demonstrated that land-atmosphere coupling is not a one-dimensional phenomenon; it exhibits multi-dimensional characteristics (Haghighi et al. 2018). Beyond moisture factors, both thermal energy and ecological factors exert a strong influence on atmospheric processes, although they have received relatively less attention (Hsu and Dirmeyer 2021; Tang et al. 2018). Surface temperature plays an essential role in determining sensible heat flux and boundary layer development, thereby influencing atmospheric temperature, humidity, and stability. Consequently, surface temperature exhibits strong coupling with near-surface temperature, humidity, and boundary layer height (Tao et al. 2019). In the Southern Great Plains of North America, due to the ecological regulation of vegetation transpiration, Leaf Area Index (LAI) demonstrates strong coupling strength with surface fluxes that surpasses that of soil moisture (Tang et al. 2018). Thermal and ecological factors not only couple with the atmosphere but also influence the spatiotemporal distribution of coupling. Coupling strength gradually intensifies with rising temperatures. While temperatures are below 0 °C, the limited energy input restricts ecosystem activity, resulting in very weak land-atmosphere coupling (Gerken et al. 2019). Generally, land-atmosphere coupling is regulated by moisture in water-scarce regions, whereas in areas with ample moisture, it is controlled by thermal and energy factors (Zscheischler et al. 2015). Besides, changes in vegetation status could alter surface moisture conditions, thereby modifying the strength of land-atmosphere coupling (Zscheischler et al. 2015). Hence, multiple land surface factors, including surface moisture, energy, and vegetation related variables, are coupled with the atmosphere. Variations in these land surface variables would lead to significant spatiotemporal heterogeneity in land-atmosphere coupling. Current research mainly focus on the coupling between individual land surface variables, like soil moisture, and the atmosphere. However, further research is required to investigate the complex interactions between multifactor land surfaces and the atmosphere, which characterize a critical aspect of land-atmosphere coupling.

The Tibetan Plateau stands as the highest-altitude and most intricately contoured plateau in the world. Its land-atmosphere coupling system significantly influences the climate patterns of East Asia, the progression of the Asian monsoon, and the atmospheric circulation in the Northern Hemisphere (Huang et al. 2023; Ma et al. 2023; Talib et al. 2021; Zhao et al. 2018). Regardless of the presence of complex topography, soil moisture notably impacts precipitation(Barton et al. 2021), while the influence of precipitation on soil moisture depends on precipitation intensity (Meng et al. 2018). Spatially, in the central and eastern part of the plateau, soil moisture in spring exhibits a positive coupling with summer precipitation, while in the western region, a negative coupling relationship is observed (Yang and Wang 2022). Seasonally, land-atmosphere coupling on the plateau is primarily influenced by snow cover during the dry season, while during the wet season, soil moisture becomes the dominant factor (Sun et al. 2021). Current research on land-atmosphere coupling in the plateau region primarily focuses on the core region of the Tibetan Plateau, with limited attention given to the plateau slopes. The northeastern slopes of the Tibetan Plateau experience frequent extreme weather and climate events, including heavy precipitation. Land-atmosphere coupling plays a crucial role in triggering precipitation events in this region. Therefore, land-atmosphere coupling is of paramount importance for understanding the mechanisms behind extreme weather and climate events in this area.

As a transitional zone between the Tibetan Plateau and the Loess Plateau, the northeastern slope of the Tibetan Plateau has a typical complex land surface characterized not only by steep topographical changes but also by highly

uneven surface conditions. Transition zones exhibit significant spatial variations in surface vegetation and highly uneven spatial distributions of land surface thermal and moisture characteristics(Ma and Ma 2016). This results in differing surface energy, moisture fluxes, and their regulating factors, leading to complexity in the forcing of the boundary layer and the free atmosphere(Fan et al. 2019). Currently, the coupling characteristics of multiple land surface factors with precipitation remain unclear in this region. This limited understanding hinders our ability to comprehend how land surface conditions regulate surface energy and moisture exchanges and their impacts on atmospheric boundary layer characteristics and even atmospheric precipitation processes in this area(Talib et al. 2023).

With these in mind, the current research uses complex correlation diagnose the land-atmosphere coupling involving multiple land surface variables (such as water, thermal, and ecological factors) and precipitation, and characterizes the spatial pattern of on the northeastern slope of the Tibetan Plateau. We also examine how coupling strength varies with changes in land surface state variables. Furthermore, we quantitatively analyze the contributions of hydrological, thermal, and ecological factors to land-atmosphere coupling, and distinguish the differences in land-atmosphere coupling strength and the primary contributing factors across various vegetation types. These efforts aim to provide a more comprehensive understanding of how land surface processes influence precipitation in the study area and deepen our knowledge of the intricate land-atmosphere feedback processes.

2 Study areas and data

2.1 Study areas

The study area encompasses the northeastern slope of the Tibetan Plateau, spanning from 33° – 39°N and 92° – 102°E (see Fig. 1). This region serves as a transitional zone between the towering altitudes of the Tibetan Plateau and the Loess Plateau, characterized by an elevation difference of nearly 3000 m. This area exhibits a diverse range of vegetation types, including high-altitude snow cover, alpine meadows, cropland, high-altitude forests, and deserts. Due to the influence of complex topography, local dynamics and thermodynamics operate highly unevenly in this region, making it one of the most complex land-atmosphere interaction zones. The complex terrain in this area fosters frequent convective activities(Ma et al. 2022), resulting in strong associations between land-atmosphere interactions and convective processes(Imamovic et al. 2017).

2.2 Data

Soil moisture selected the SMC (Soil Moisture in China) dataset(Meng et al. 2021). The soil moisture data spans from 2002 to 2018, in monthly temporal and 0.05° spatial resolution. It is produced by from three passive microwave remote sensing products: the Japan Aerospace Exploration Agency's Microwave Scanning Radiometer - Earth Observing System (AMSR-E) and the Advanced Microwave Scanning Radiometer 2 (AMSR2) Level 3 soil moisture data, and SMOS-IC (Soil Moisture and Ocean Salinity designed by the Institut National de la Recherche Agronomique, INRA, and Centre d'Etudes Spatiales de la BIOsphère, CESBIO) products–calibrated with a consistent model in combination with ground observation data. Overall, the downscaled soil moisture (SM) products were consistent with the in-situ measurements ($R > 0.78$) and exhibited a low root mean square error (RMSE < 0.05 m^3/m^3).

Land surface temperature data selected the Terra Moderate Resolution Imaging Spectroradiometer (MODIS) Land Surface Temperature/Emissivity 8-Day (MOD11A2) Version 6.1 product(Wan 2014). This product provides an average 8-day per-pixel Land Surface Temperature and Emissivity (LST&E) with a 1 km (km) spatial resolution.

LAI selected MOD15A2H product(Wenze et al. 2006), with a temporal resolution of 8-day and spatial resolution of 500 m. The LAI variable defines the number of equivalent layers of leaves relative to a unit of ground area. The accuracy has been assessed over a widely distributed set of

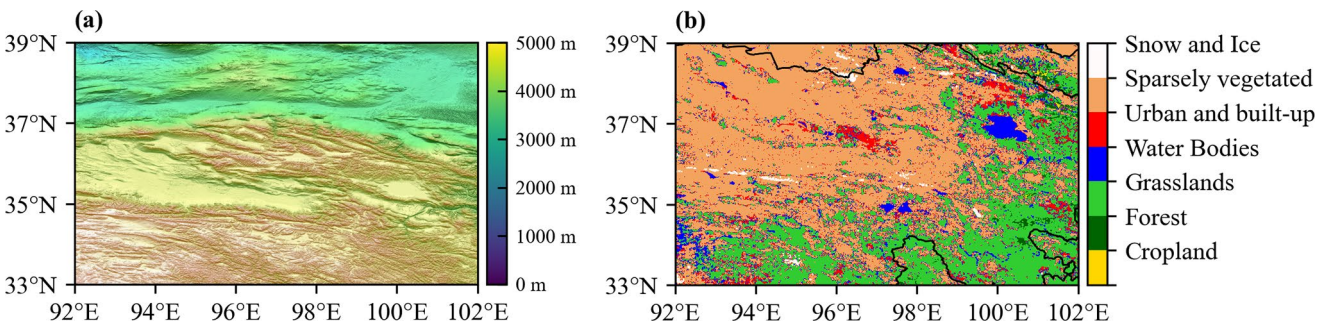

Fig. 1 Topography (**a**, red rectangle) and land cover type (**b**) of the study area

locations and time periods via several ground-truth and validation efforts.

The surface evapotranspiration data used in this study were obtained from a global gridded synthesis ET estimate, the Derived Optimal Linear Combination Evapotranspiration (DOLCE) (Hobeichi et al. 2018). DOLCE ET is a blended dataset constrained by observations, combining four global evapotranspiration datasets: ERA5-land, FLUXCOM METEO + RS, GLEAM v3.5a, and GLEAM v3.5b. The combination of these parent datasets is based on their performance in estimating flux tower evapotranspiration, taking into account their error dependencies. The weights assigned to the parent datasets vary with season (December to May/June to November) and climatic zones. The latest version, DOLCE -ET V3.0, also provides estimates of the temporal variability of its uncertainty errors. DOLCE -ET V3.0 has a monthly temporal resolution and a spatial resolution of 0.25°, covering the period from 1980 to 2018 and encompassing global land areas.

Sensible heat fluxes selected the Global Land Data Assimilation System (GLDAS, version 2.1) product(Rodell et al. 2004). GLDAS ingests satellite- and ground-based observational data products, using advanced land surface modeling and data assimilation techniques, in order to generate optimal fields of land surface states and fluxes. The simulations of the Noah land surface models was used in this study. The data spans 2000-present with a monthly 0.25 -degree resolution.

Precipitation uses China Meteorological Forcing Dataset (CMFD)(Yang and He 2019). The data set was developed by the Institute of Tibetan Plateau Research, Chinese Academy of Sciences. CMFD used Princeton reanalysis data, GLDAS (global land data assimilation system) data, GEWEX-SRB (the global energy and water exchanges) radiation data, and TRMM (tropical rainfall measuring mission) precipitation data as background fields, and merged the conventional meteorological observation data of China Meteorological Administration (CMA) to produce a regional high spatial and temporal resolution dataset. The dataset has a temporal resolution of from 3-hour to month and a spatial resolution of 0.1°, with a spatial range of 60°- 140°E and 15–55°N.

Landcover classification uses MODIS product MCD12C1(Sulla-Menashe et al. 2019). The data sets have a spatial resolution of 0.25° and 17 classifications.

3 Methods

3.1 Data processing

The time period 2003–2018 was selected as the study period because of the temporal overlap of all data. Except for MODIS land surface temperature and LAI data have a temporal resolution of 8-day, other data have a temporal resolution of a month. Thus, MODIS land surface temperature and LAI data were linearly interpolated into monthly timescale. As most of the data had a spatial scale of 0.25°, all other data were regridded to 0.25°. The seasonal cycles and long-term trends of monthly data were removed before calculation of the coupling strength index and contribution.

3.2 Coupling strength index

There are numerous indices to measure coupling strength, with each focusing on different aspects. In this paper, correlation coefficients are utilized to diagnose land-atmosphere coupling strength. A higher correlation coefficient indicates stronger coupling, with the sign (positive or negative) representing the direction of the coupling. Using correlation coefficients as an indicator of coupling strength offers the advantage of comparing the strengths of coupling between different variables. Bivariate coupling, e.g. soil moisture-latent heat flux coupling, is calculated using the bivariate Pearson correlation coefficient. When considering the synergistic coupling strength of multiple factors with a particular variable, it can be achieved by calculating their complex correlation coefficients (Tang et al. 2018). In this study, the synergistic coupling between several land surface variables (soil moisture, surface temperature, and LAI) and surface fluxes, as well as the coupling between sensible heat, latent heat flux, and precipitation, is calculated using complex correlation coefficients.

3.3 Contribution of individual variables

When considering the synergetic impact of multiple factors on a specific variable, it is enlightening to quantify the contributions of each factor to that variable. The contributions of individual factors can be determined using multiple linear regression (Tang et al. 2018). As an illustrative example, we consider the assessment of the contributions of soil moisture, surface temperature, and Leaf Area Index (LAI) to latent heat. Firstly, a linear regression equation is derived through linear fitting, establishing the relationship between latent heat flux and these three surface variables.

$$LE = \mathrm{b}_0 + b_{sm} * sm + b_{ts} * ts + b_{LAI} * LAI \tag{1}$$

Subsequently, the contributions of each surface variables can be calculated using the following equation:

$$B_{sm} = b_{sm} * \delta_{sm}/\delta_{LE} \tag{2}$$

$$B_{\mathrm{ts}} = b_{ts} * \delta_{ts}/\delta_{LE} \tag{3}$$

$$B_{LAI} = b_{LAI} * \delta_{LAI}/\delta_{LE} \quad (4)$$

Here, B_{xx} represents the contribution of the *xx* (*xx* represents sm, ts, or LAI), b_{xx} stands for the fitted coefficient of the *xx*, and δ_{xx} denotes the standard deviation of *xx*.

Likewise, the same method can be applied to compute the contributions of three surface variables to sensible heat flux, as well as the contributions of sensible heat flux and latent heat flux to precipitation.

3.4 Definition of convective precipitation

Previous studies indicate that convective precipitation primarily occurs between the afternoon and early evening (Petrova et al. 2018; Taylor et al. 2012). This precipitation is mainly generated by isolated convection or weak to moderate intensity mesoscale convective systems (Hu et al. 2021). Therefore, following Taylor's approach, convective precipitation is defined as follows: Cumulative precipitation between 12:00 and 21:00. This definition is easy to implement but may include some large-scale precipitation. Exclusion of days with precipitation between 06:00 and 12:00 to eliminate the influence of large-scale precipitation.

4 Results

4.1 Spatial and temporal variations of land surface states, surface fluxes, and precipitation

4.1.1 Land surface states

The complexity of the underlying surface on the northeastern slope of the Tibetan Plateau results in a highly heterogeneous land surface. In this section, we first analyze the spatial variations in surface water, thermodynamics, and ecological conditions. Figure 2 illustrates the spatial distribution of climatology and temporal variations in surface soil moisture (sm), surface temperature (Ts), and Leaf Area Index (LAI) within the study area.

Regarding the spatial distribution of climatology of the surface variables, it can be observed that soil moisture generally increases from north to south (Fig. 2a), which corresponds to the northern regions being predominantly desert and Gobi, while the southern regions are characterized by grasslands or alpine forests. Furthermore, the areas surrounding Qinghai Lake also exhibit relatively high soil moisture levels, primarily influenced by the replenishment of lake water. The spatial distribution of surface temperature exhibits a broadly contrasting pattern to that of soil moisture (Fig. 2c), with higher temperatures prevailing in the northern regions and lower temperatures in the southern regions. The northwest part, Qaidam Basin, is characterized by arid deserts, while the northeast corner consists of Gobi areas, both of which exhibit significantly elevated surface temperatures. In contrast, the southern portion of the study area, covering the Qinghai Plateau, features alpine grasslands and high-altitude forests, resulting in relatively lower surface temperatures. There is significant spatial variation in the Leaf Area Index (LAI), increasing from northwest to southeast (Fig. 2e). In the arid desert regions of the northwest, vegetation is extremely sparse, leading to missing LAI data. In contrast, the northeastern Qilian Mountain region and the southeastern Yellow River source area exhibit exceptionally high LAI values, indicating dense vegetation cover in these areas. The distribution of LAI closely resembles that of soil moisture, highlighting the dependence of vegetation on moisture conditions in the northeastern slope region of the Tibetan Plateau. Clearly, the distribution of surface water, thermal, and ecological factors in the northern slope region of the plateau is profoundly heterogeneous, characterized by strong local variations.

When examining the distribution of relative variation, the relative variations in soil moisture and surface temperature are broadly consistent with their spatial pattern of climatology. The relative variation of LAI is relative small in areas with sparse vegetation, primarily in the northwest edge region, and relative large in areas with moderate to dense vegetation.

4.1.2 Surface fluxes

Within land-atmosphere interactions, land surface states facilitate the exchange of matter and energy with the atmosphere through surface fluxes. Figure 3 presents the climatology and spatial distribution of latent and sensible heat fluxes. Latent heat flux increases from northwest to southeast, with minimal values in the northwestern desert regions, approaching to 0 W/m^2, and the maximum values reaching approximately 50 W/m^2 in the eastern Qinghai Lake, Qilian Mountains, and the eastern Tibetan Plateau. Constrained by the surface energy balance, the spatial distribution of sensible heat flux presents an inverse pattern to that of latent heat flux. It decreases from northwest to southeast, with the maximum values (approximately 60 W/m2) observed in the northwestern desert regions and the minimum values (around 30 W/m2) found in areas around Qinghai Lake, the Qilian Mountains, and the Three-River-Source region.

The spatial distribution of variability of latent heat flux exhibits a pattern opposite to that of climatology of latent heat flux, while variability of sensible heat flux decreases from north to south. The relatively small variability in sensible heat flux, compared to the larger variability in latent heat flux, is due to the simultaneous influence of moisture

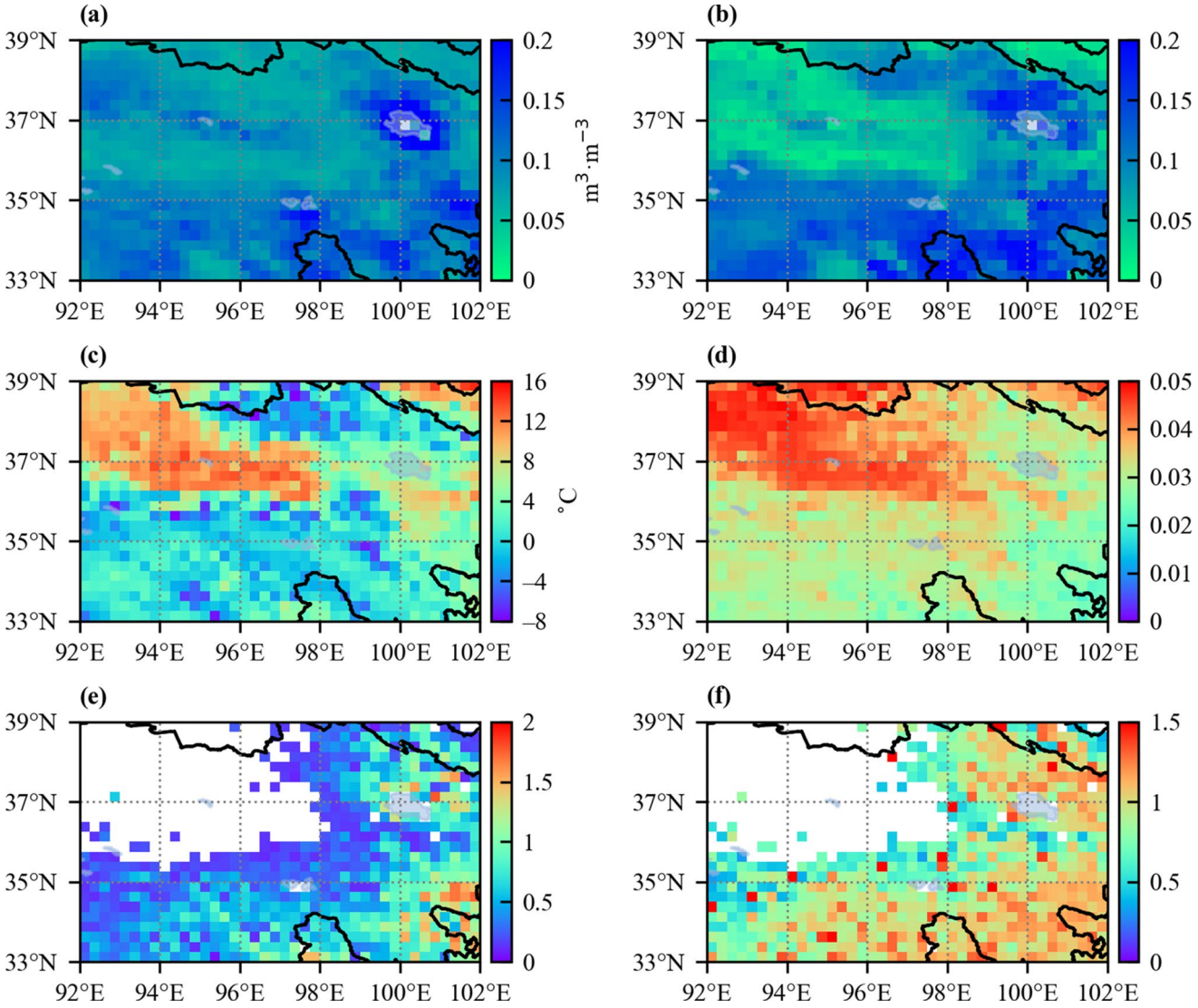

Fig. 2 Spatial distribution of means (**a**, **c**, **e**) and variability (**b**, **d**, **f**) of soil moisture (sm), surface temperature (Ts), and leaf area index (LAI) on the northern slope of the Tibetan Plateau

and thermal energy factors on latent heat flux, making its influencing mechanism more complex. Consequently, the spatial heterogeneity in surface conditions contributes to pronounced spatial disparities in surface fluxes and their variations within the study area.

4.1.3 Precipitation

The spatial distribution of precipitation climatology and its variability in the study area is illustrated in Fig. 4. Precipitation climatology increases from northwest to southeast, with the lowest values of a few millimeters in the northwest Tarim Basin and the highest values of approximately 70 mm in the southeastern Yellow River source region. The relative variability of monthly precipitation exhibits an opposing spatial pattern, generally decreasing from northwest to southeast.

Precipitation shows relatively higher relative variability in the Qaidam Basin, Qilian Mountains, and the western part of the Tibetan Plateau, whereas regions with greater precipitation in the southeast display relatively lower relative variability. Thus, it is apparent that the spatiotemporal distribution of precipitation on the northeastern slope of the Tibetan Plateau is notably uneven. Further understanding is required regarding the contribution of heterogeneous land surface state to this uneven precipitation distribution.

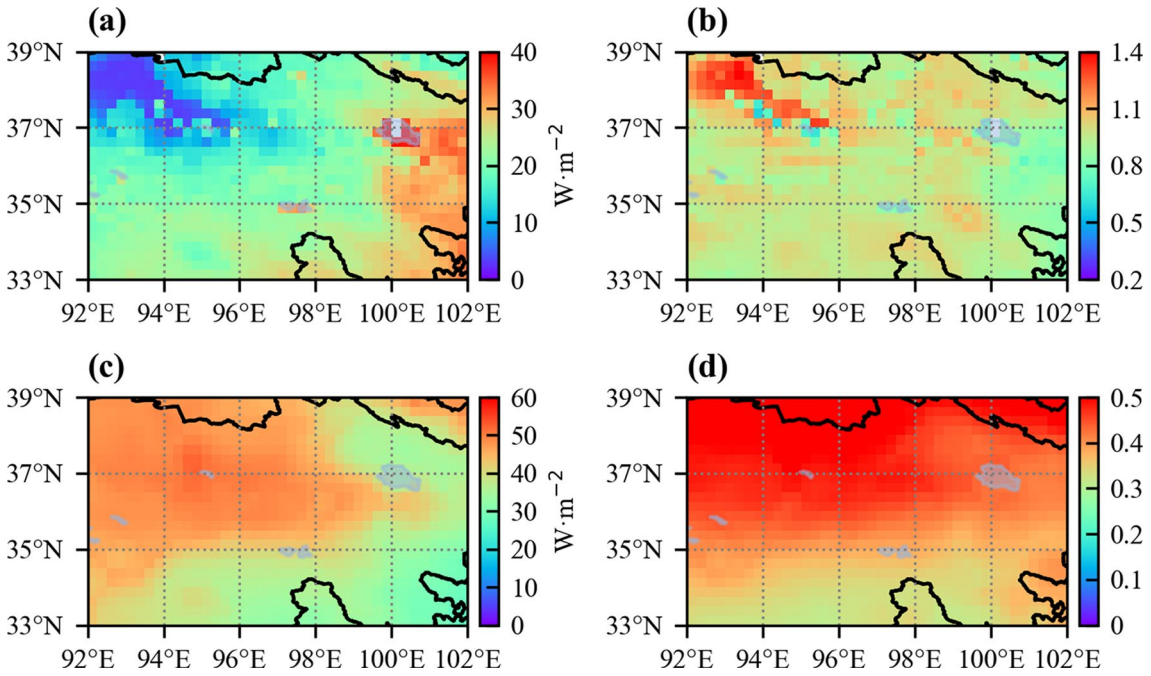

Fig. 3 Spatial distribution of mean (**a**, **c**) and standard deviation (**b**, **d**) of LE and H on the northeastern slope of the Tibetan Plateau

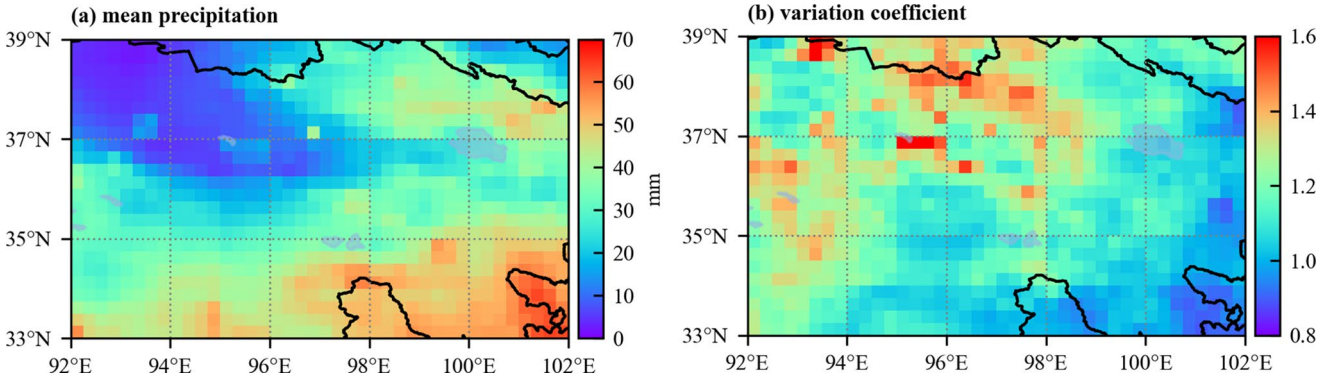

Fig. 4 Spatial distribution of mean (**a**) and variability (**b**) of precipitation on the northeastern slope of the Tibetan Plateau

4.2 Spatial distribution of land-atmosphere coupling

4.2.1 Spatial distribution of surface coupling

Using correlation coefficients as coupling indicators not only reflects the coupling relationship between two physical quantities but also allows for comparisons of different coupling strengths. Land-atmosphere coupling can be divided into two stages: land surface variables to surface flux coupling and surface flux to precipitation coupling. We begin by characterizing the spatial distribution of the coupling of land surface variable to surface fluxes.

Soil moisture-latent heat coupling (sm-LE-C) generally exhibits a dipole-shaped pattern, with the northwest part of the study area being positive and the southeast part being negative. Notably, these positive and negative coupling regions align closely with the areas of low and high soil moisture values (see Fig. 5a). In the Tarim Basin and surrounding areas, sm-LE-C coupling reaches around 0.8. The positive sm-LE-C coupling region indicates that latent heat is limited by moisture in these areas, while the negative coupling region suggests that latent heat is limited by energy.

Soil moisture-sensible heat coupling (sm-H-C) predominantly reveals negative values across most of the study area. Positive coupling is observed only in regions with higher soil moisture near Qinghai Lake and the Yellow River source area (see Fig. 5b). The strongest negative coupling (-0.8) occurs in the Qilian Mountains and the western and central part of the Qinghai Plateau, which represents a transitional zone from desert to humid conditions in the Three Rivers Source region. sm-LE-C and sm-H-C generally

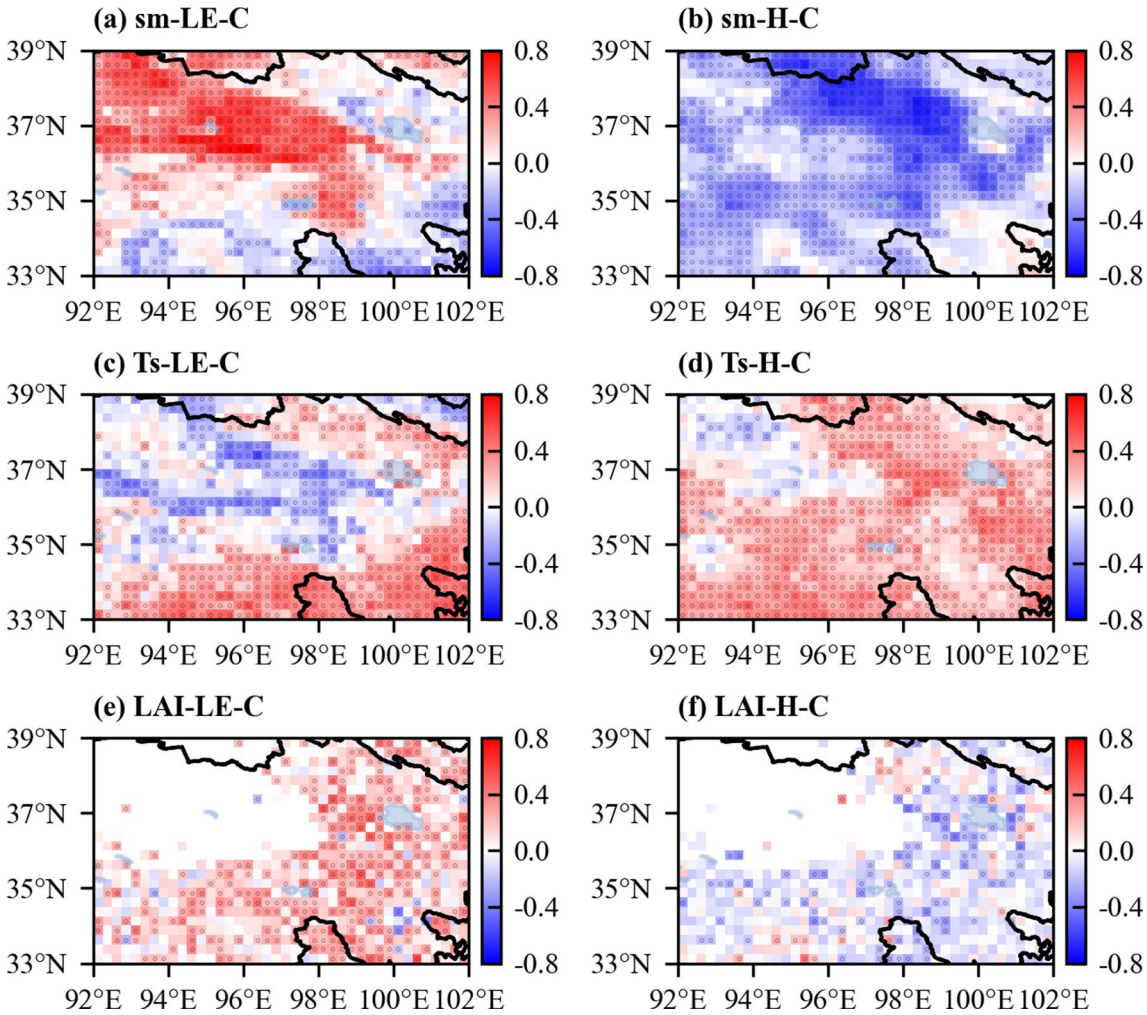

Fig. 5 Spatial distribution of coupling between soil moisture, surface temperature, LAI and LE, H: (**a**) soil moisture-LE coupling (sm-LE-C), (**b**) soil moisture-H coupling (sm-H-C), (**c**) surface temperature-LE coupling (Ts-LE-C), (**d**) surface temperature-H coupling (Ts-H-C), (**e**) LAI-LE coupling (LAI-LE-C), (**f**) LAI-H coupling (LAI-H-C), shaded dots indicate passing $p < 0.01$ significance test

exhibit opposite signs across most regions, illustrating the constraining role of surface energy balance in land-atmosphere interactions. With limited available energy, when more energy is allocated to LE due to larger sm, H becomes smaller. Consequently, variations in soil moisture lead to opposite changes in LE and H.

Surface temperature-latent heat coupling (Ts-LE-C) exhibits a spatial distribution pattern opposite to sm-LE-C, with predominantly negative coupling in the northwest region and positive coupling in the southeast and Qilian Mountains region (Fig. 5c). Ts mainly represents surface thermal energy. In the northwestern moisture-limited region, Ts has a relatively minor influence on LE, resulting in weak negative coupling in Ts-LE-C. Conversely, in the southeastern energy-limited region, Ts exerts a more substantial driving effect on LE, leading to a notably strong positive coupling in Ts-LE-C (approximately 0.5). It is worth noting that the negative coupling of Ts-LE-C actually reflects the increase in LE due to increased soil moisture, leading to a decrease in Ts. As Ts consistently drives H, the surface temperature-sensible heat coupling (Ts-H-C) coupling is positive throughout the study area, with smaller values in the northwestern desert and Qilian Mountains regions and coefficients of approximately 0.4–0.5 in other regions (Fig. 5d).

The leaf area index-latent heat coupling (LAI-LE-C) is primarily positive throughout the study area (Fig. 5e), with stronger regions reaching approximately 0.5. Conversely, the leaf area index-sensible heat coupling (LAI-H-C) mainly exhibits negative coupling (Fig. 5f), with stronger regions reaching approximately −0.4. This suggests that increased vegetation enhances transpiration, promoting LE, while conversely, the cooling effect resulting from increased LE under enhanced vegetation suppresses H. LAI-LE-C and LAI-H-C generally strengthen from the northwest to the southeast, indicating weaker coupling under conditions of poor vegetation and stronger coupling under moderate to

good LAI conditions. There is no LAI data for the northwestern desert and Gobi regions.

4.2.2 Synergetic coupling of multiple surface variables with fluxes

As seen from the previous analysis of the coupling between individual land surface elements and surface fluxes, there are significant spatial variations in the coupling of different land surface elements with LE or H. This highlights substantial spatial differences in the coupling of moisture, thermal, and ecological factors with surface fluxes. Although the individual coupling of land surface water, heat, and ecological factors with surface fluxes reflects the coupling between the land surface and surface fluxes, each of them is only part of land-atmosphere coupling. A more comprehensive description of local land-atmosphere coupling requires considering the combined impact of these three factors on surface fluxes, i.e., the synergistic coupling of water, heat, and ecological factors with surface fluxes. Therefore, we employed the complex correlation coefficient to analyze the synergistic coupling of LE and H with water (sm), thermal (Ts), and ecological factors (LAI).

Figure 6 presents the synergistic coupling of sm, Ts, and LAI with LE and H. The synergetic coupling of sm, Ts, LAI and LE (S-LE-C) is stronger in the northwest desert region than other areas, reaching around 0.8, and increases from northwest (less than 0.2) to southeast (0.4–0.8) across other areas. The synergetic coupling of sm, Ts, LAI and H (S-H-C) is relatively low (< 0.2) in the northwest desert area, the Three-River Source region, and areas around Qinghai Lake. In other regions (including the Qilian Mountains and the central-western part of the Qinghai Plateau, transitioning from desert to humid regions in the Three-River Source area), the S-H-C values are much higher (0.5–0.8). By comparing the synergetic coupling and individual coupling, it is evident that synergetic coupling strength is significantly enhanced compared to individual coupling strength (Fig. 5). It effectively highlights regions characterized by strong couplings of individual factors. This indicates that the synergetic coupling provides a more comprehensive representation of the combined influence of surface water, heat, and biological factors on surface fluxes.

4.2.3 Contribution of each surface variable to fluxes

Multivariate coupling characterizes the synergistic effects of multiple surface factors on surface fluxes. Further analysis is required to determine the specific contributions of each factor to surface fluxes. Figure 7 illustrates the contributions of three surface factors to latent and sensible heat fluxes. In regions with low soil moisture (sm), sm has a strong positive contribution to latent heat flux (LE) and a strong negative contribution to sensible heat flux (H). Surface temperature (Ts) makes a significant positive contribution to LE in more humid areas and areas with higher leaf area index (LAI). The positive contribution of Ts to H is relatively small and exhibits minimal spatial variation. LAI exerts a positive contribution to LE and a negative contribution to H, with larger contributions in areas characterized by moderate to high LAI. The contributions of each surface factor to the convergence coupling degree exhibit spatial distributions similar to their individual coupling with surface fluxes. This indicates that synergetic coupling effectively integrates the impacts of diverse surface factors on surface fluxes and comprehensively represents the control exerted by surface moisture, temperature, and vegetation status on surface fluxes.

4.3 Distribution of atmospheric stage of land-atmosphere coupling

4.3.1 Spatial distribution of atmospheric coupling

The surface flux-precipitation coupling is the second stage of land-atmosphere coupling. Figure 8 illustrates the coupling

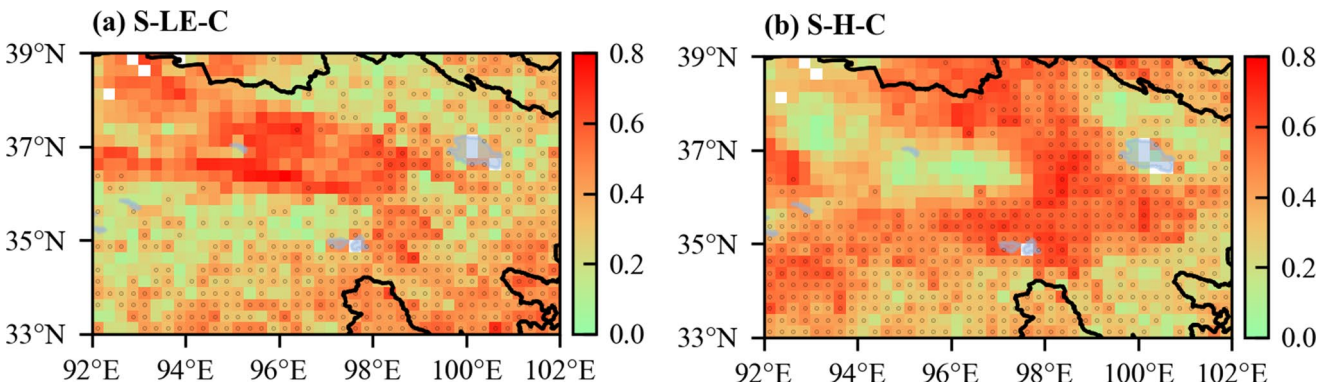

Fig. 6 Spatial distribution of synergetic coupling of land-surface multifactor to surface fluxes, (**a**) for the synergistic coupling of sm, Ts, and LAI with LE (S-LE-C), (**b**) for the synergistic coupling of sm, Ts, and LAI with H (S-H-C) (shaded dots indicate passing $p < 0.01$ significance test)

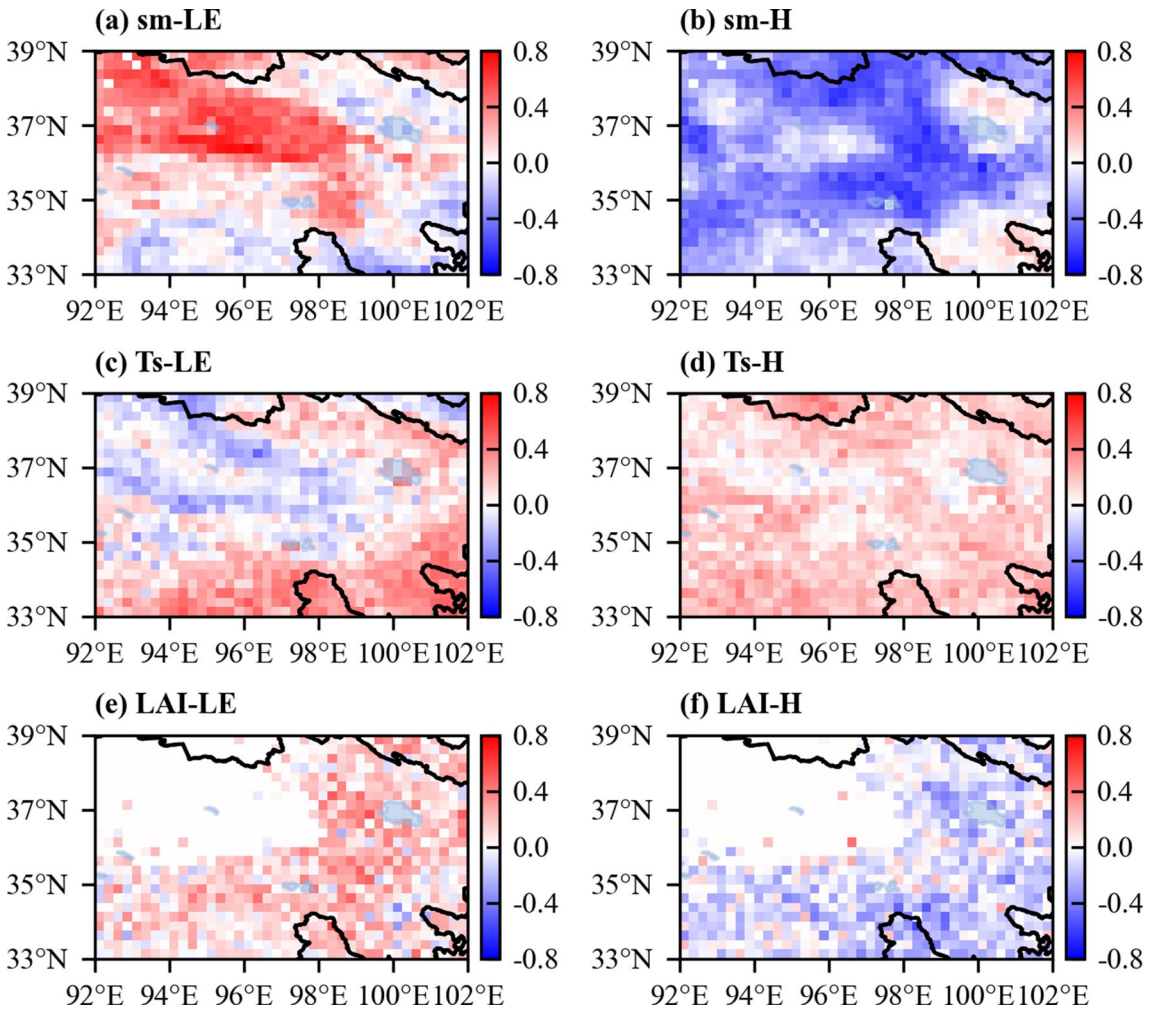

Fig. 7 Spatial distribution of the contribution of land surface variables soil moisture (sm), surface temperature (Ts), and LAI to surface fluxes LE and H

between latent and sensible heat fluxes and precipitation. In the study area, latent heat flux-precipitation coupling (LE-P-C) is positive in the northern regions, which are mainly characterized by sparse vegetation such as desert and Gobi areas, and negative in the southern regions, encompassing areas near Qinghai Lake and most parts of the Tibetan Plateau (Fig. 8a).

Sensible heat-precipitation coupling (H-P-C) exhibits an approximately opposite distribution pattern (Fig. 8c), with negative values in the northern regions and positive values in the southern regions. The spatial patterns of LE-P-C and H-P-C correspond to areas with lower and higher vegetation cover, respectively, reflecting drier conditions in the northern regions and wetter conditions in the southern regions. The positive LE-P-C and negative H-P-C coupling in the northern regions reflect a significant positive contribution of evaporation to precipitation in these drier areas, implying that increased evaporation leads to enhanced moisture and, consequently, increased precipitation.

In the southern regions, positive H-P-C and negative LE-P-C coupling indicate that boundary layer thermodynamics play a dominant role in contributing to precipitation. Figure 9 illustrates that increased sensible heat leads to higher boundary layer heights, enhancing atmospheric instability, atmospheric instability, characterized by larger Convective Available Potential Energy (CAPE) and lower Convective Inhibition (CIN), thereby promoting convection and increasing precipitation. However, in terms of coupling strength, whether positive or negative, it is generally not strong, even in relatively significant areas, it's only around 0.3–0.4.

4.3.2 Synergetic coupling of latent and sensible heat flux with precipitation

Since H and LE can each only reflect a portion of the impact of surface fluxes on precipitation, comprehensively studying the effect of surface fluxes on precipitation, similar to

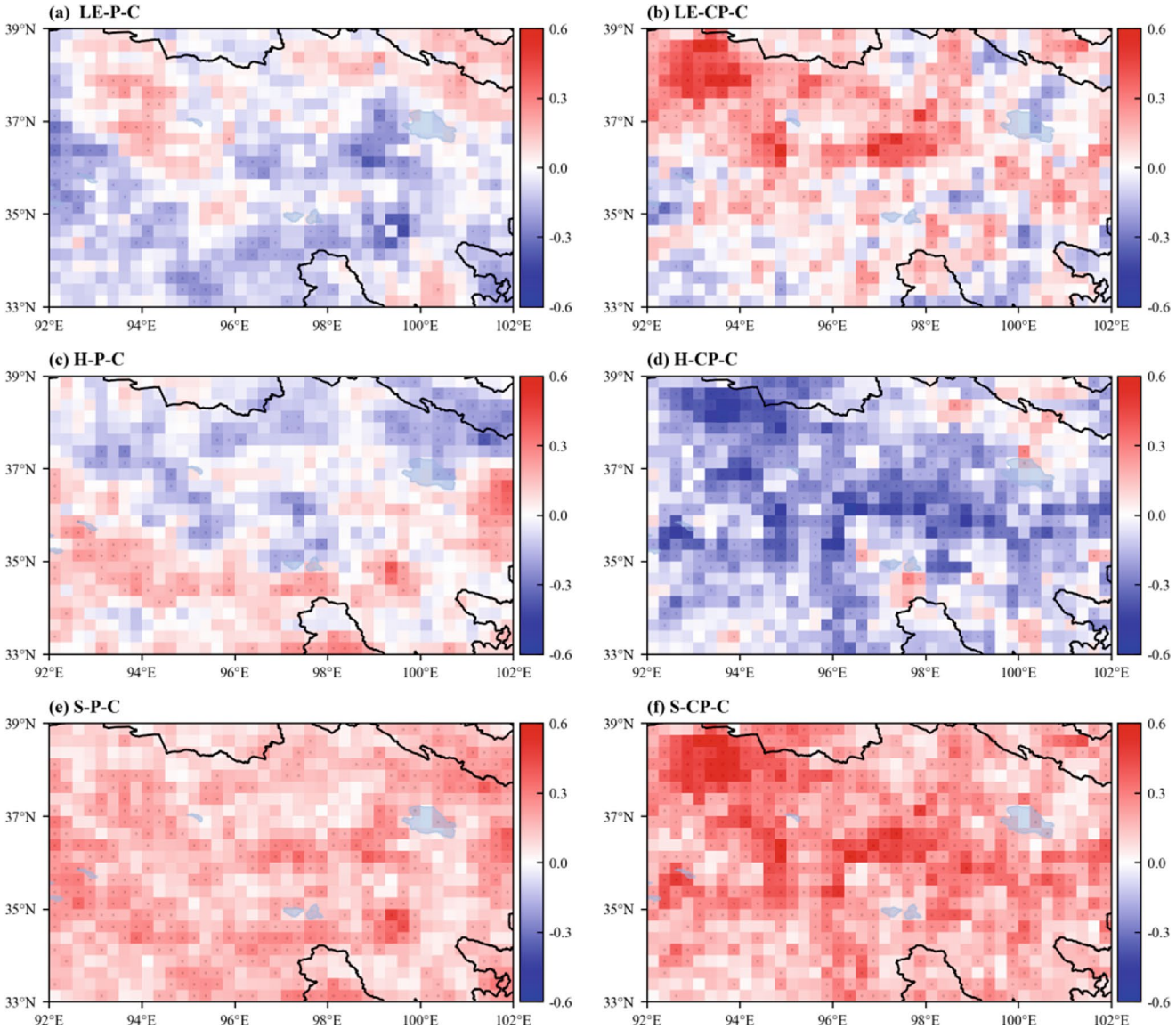

Fig. 8 Spatial distribution of coupling of surface fluxes to total precipitation and convection precipitation, (**a**) for LE-precipitation coupling (LE-P-C), (**b**) for LE-convection precipitation coupling (LE-CP-C), (**c**) for H-precipitation coupling (H-P-C), (**d**) for H-convection precipitation coupling (H-CP-C), (**e**) for synergetic coupling between surface fluxes and precipitation (S-P-C), (**f**) for synergetic coupling between surface fluxes and convection precipitation (S-CP-C), shaded dots indicate passing $p < 0.01$ significance test

multi-surface factor-surface fluxes synergetic coupling, involves defining a synergetic coupling for the combined impact of H and LE on P. Figure 8e shows the spatial distribution of synergetic coupling (S-P-C) between LE, H, and P across the study area. It's evident that when considering both H and LE, the coupling strength significantly increases due to the combined effect of sensible and latent heat on precipitation. The correlation coefficients reach around 0.4 in most regions. However, despite this enhancement, the coupling strength only amounts to a moderate correlation coefficient even in regions with strong coupling. H and LE together can explain only approximately 16% (R^2) of the variation in precipitation.

From the analysis above, it's evident that the coupling between H, LE, and P is relatively weak in the study area, approximately around 0.4. This because the influence of surface fluxes on precipitation depends on precipitation components. Since surface-triggered convective precipitation often occurs in the afternoon, further analysis was conducted on the coupling between H, LE, and afternoon (15:00–21:00 local time) convective precipitation (CP). LE shows a more robust coupling with convective precipitation (LE-CP-C) compared to total precipitation (LE-P-C), and this coupling is more extensive, with most regions in the area demonstrating positive coupling (Fig. 8b). H shows a stronger negative coupling with convective precipitation (H-CP-C) compared

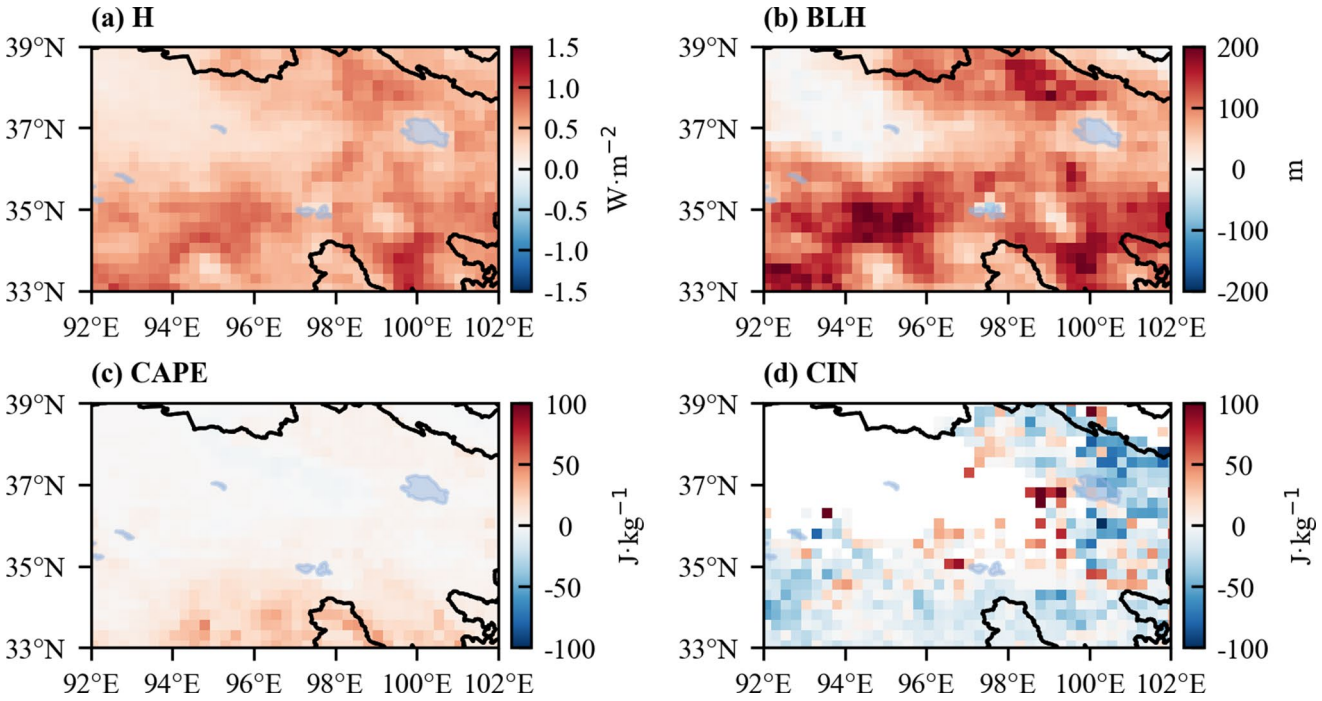

Fig. 9 Anomaly of sensible heat flux (H), boundary layer height (BLH), Convective Available Potential Energy (CAPE) and Convective Inhibition (CIN) under positive sensible heat flux condition

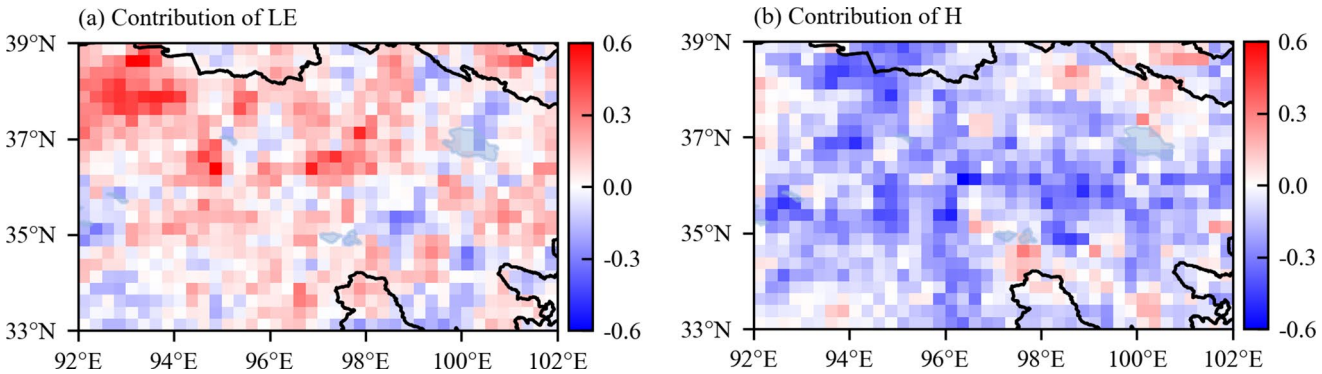

Fig. 10 Spatial distribution of contributions of latent (**a**, LE) and sensible (**b**, H) heat to afternoon convective precipitation

to total precipitation (H-P-C), and the study area predominantly exhibits negative coupling (Fig. 8d).

When considering both H and LE, the regional synergetic coupling (S-CP-C) weakens from northwest to southeast across the study area. Notably, S-CP-C increases from the original total precipitation coupling (S-P-C) of 0.4 to 0.6, and most regions pass the significance test (Fig. 8f). This indicates that H and LE make significant contributions to afternoon convective precipitation in the study area. Comparatively, the atmospheric coupling stage exhibits apparent lower coupling levels when contrasted with the land surface coupling stage (regions of higher strength ranging from 0.6 to 0.8).

Further analysis was conducted on the contributions of land surface fluxes LE and H to afternoon convective precipitation (CP) (Fig. 10a, b). Overall, positive contributions of LE to CP are larger in most regions of the study area, with the northwest being stronger than the southeast. H, on the other hand, makes negative contributions to CP, and its spatial distribution in terms of intensity is roughly similar to that of LE's contribution.

When examining the spatial distribution of contribution intensity, it's evident that LE and H exhibit consistent patterns but with opposite signs regarding their contributions to CP. This is closely linked to their complementary roles in the surface energy balance. Specifically, larger LE leads to smaller H, resulting in greater CP. This suggests that LE is the primary driver of CP in the study area.

4.4 Factors regulating spatial differences in land-atmosphere coupling strength

4.4.1 Changes in land-atmosphere coupling with surface factors

As analyzed above, land-atmosphere coupling exhibits significant spatial variations. In this section, we will explore the relationship between spatial differences in land-atmosphere coupling and the climatological distribution of surface factors. Figure 11 illustrates the relationship between surface synergetic coupling and the climatology of surface factors. As soil moisture increases, the synergy coupling of latent heat flux (S-LE-C) initially increases and then decreases, keeping a relatively strong level when soil moisture is greater than the 0.2 range. The synergy coupling of sensible heat flux (S-H-C) shows a decreasing trend with increasing soil moisture, staying a relatively weak level after soil moisture exceeds 0.15. The influence of surface temperature on S-LE-C and S-H-C is relatively weak. Despite significant variations in surface temperature (ranging from −8 to 10 °C), S-LE-C exhibits a weak increasing trend, while S-H-C shows only minor fluctuations. LAI has a more pronounced impact on surface synergy coupling. As

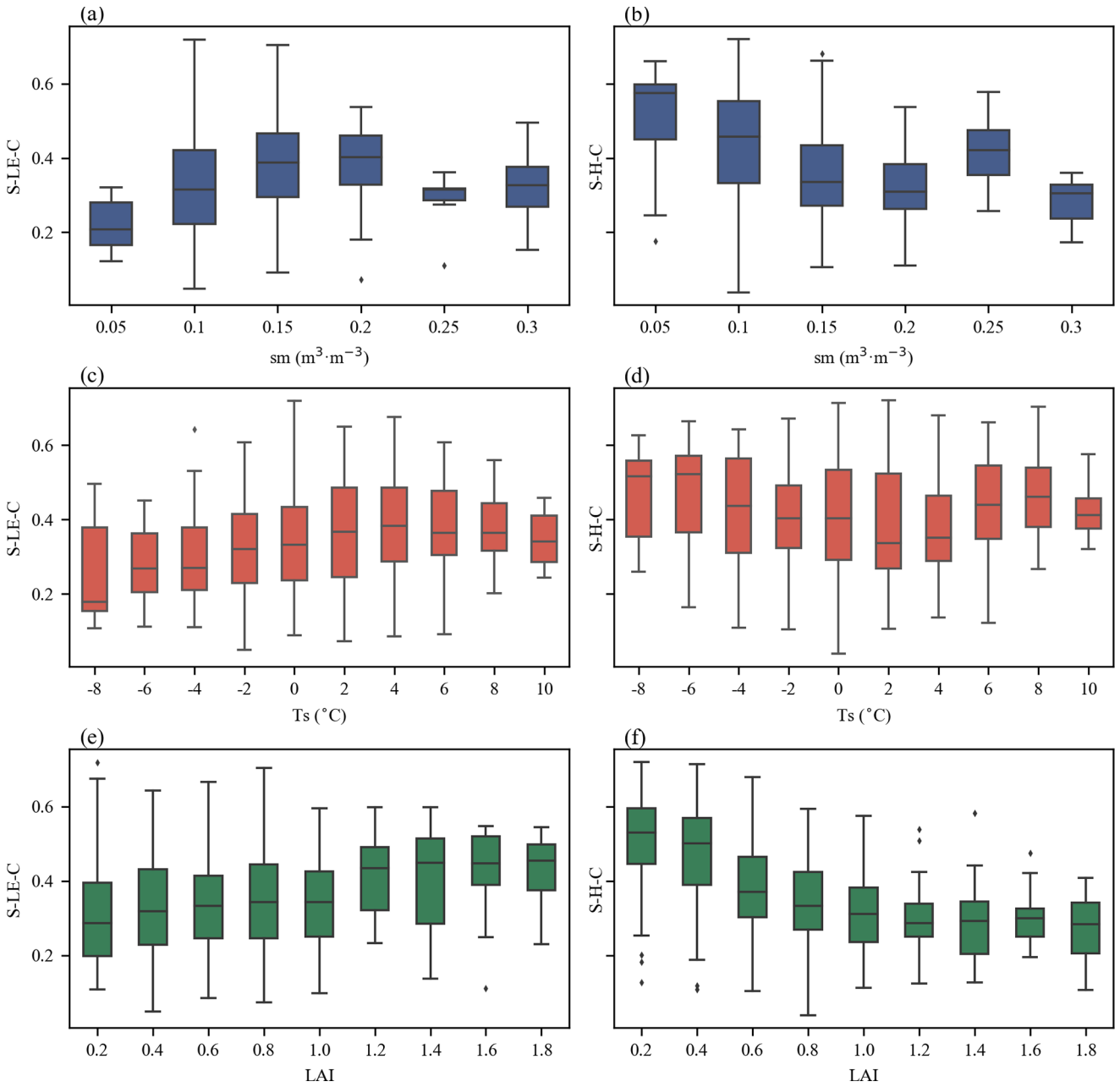

Fig. 11 Variation of surface synergetic couplings (S-LE-C and S-H-C) with surface factors (soil moisture, temperature and LAI)

LAI increases, S-LE-C gradually strengthens, while S-H-C gradually weakens. Therefore, the spatial differences in surface stage of land-atmosphere coupling are primarily influenced by soil moisture and LAI, with contrasting response patterns between latent heat flux (LE) and sensible heat flux (H) to changes in soil moisture and LAI.

Figure 12 illustrates the relationship between synergistic coupling (S-CP-C) of atmospheric coupling stage and surface factors. S-CP-C exhibits an initial increase followed by a decrease with increase in soil moisture, with the highest coupling observed within the soil moisture range of 0.1–0.15. S-CP-C strengthens as surface temperature increases, especially when the temperature is above 8 °C, exhibiting a relatively strong coupling. S-CP-C shows a decreasing trend as vegetation LAI increases, with stronger coupling when LAI is below 0.4. Considering the two-step land-atmosphere coupling, the impact of soil moisture and surface temperature on S-LE-C is similar to their impact on atmospheric coupling. While the effect of LAI on S-H-C is similar to its effect on atmospheric coupling. This reflects the impact of spatial variations in surface factors on the land-atmosphere coupling chain. Spatial differences in soil moisture and surface temperature mainly affect the surface factor-latent heat flux-precipitation coupling chain, while LAI primarily influences the surface factor-sensible heat flux-precipitation coupling chain.

4.4.2 Differences in land-atmosphere coupling in different vegetation ecosystems

The substantial spatial variations in surface properties in the study area are linked to the diverse land surface cover types, which include cropland, grassland, forest, and sparse vegetation. Different land surface cover types exhibit unique surface properties. therefore, this section analyzes the differences in land-atmosphere coupling and the contributions of various surface factors under different cover types.

First, the differences in surface synergy coupling and the contributions of various factors under different cover types were examined (Fig. 13). S-LE-C is stronger in forest compared to cropland, grassland, and sparse vegetation. This is associated with higher soil moisture and LAI in forested areas, as regions with greater soil moisture and LAI tend to have stronger S-LE-C coupling. S-H-C is strongest in areas with sparse vegetation, followed by cropland and grassland, with forests having the weakest values. This is related to the inverse relationship between soil moisture, LAI, and S-H-C, where regions with larger soil moisture and LAI tend to have weaker S-H-C values (Fig. 11).

In terms of the contributions of various surface factors to LE, soil moisture has a relatively large positive contribution in forested and sparsely vegetated areas, while its positive contribution is much smaller in cropland and grassland. Surface temperature makes a certain contribution in forested and grassland areas, but its contribution is relatively small in cropland and sparsely vegetated areas. LAI exhibits the highest contribution in cropland, followed by grassland, with minimal contributions in forests and sparse vegetation areas. Regarding the contributions of different factors to H, soil moisture has a relatively large negative contribution in cropland, followed by grassland, while it has a significant positive contribution in forests. The contributions of surface temperature and LAI are much smaller compared to soil moisture. Surface temperature makes a larger contribution in grasslands, while its contribution is small in cropland and sparse vegetation areas. LAI has a certain negative

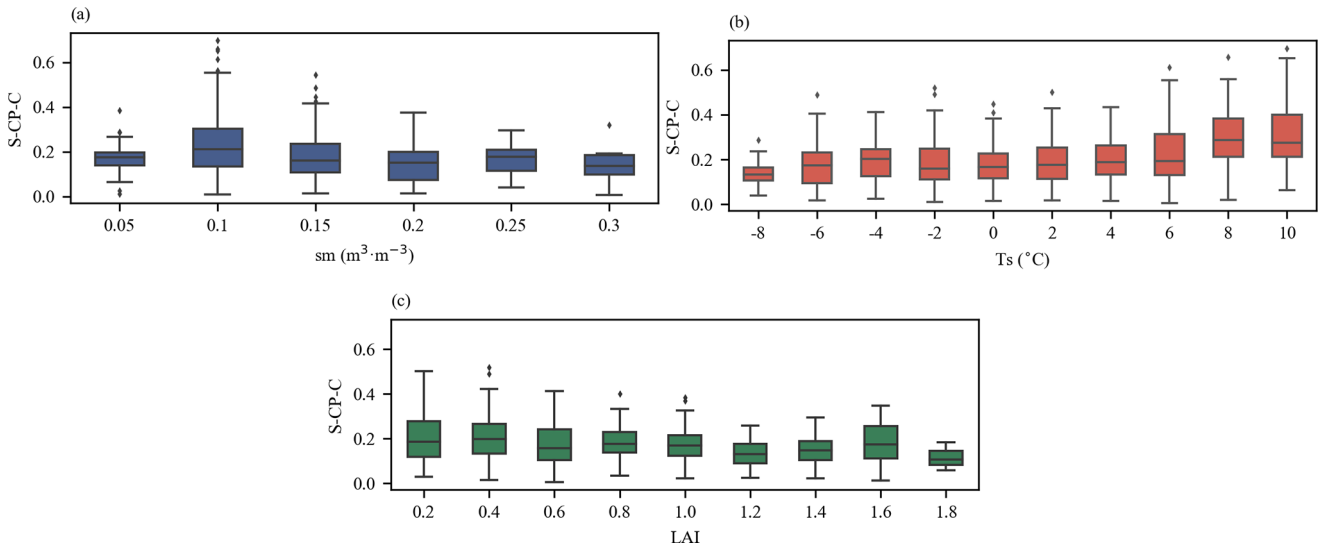

Fig. 12 Variation of atmospheric synergetic coupling (S-CP-C) with surface factors, (**a**), (**b**), and (**c**) for soil moisture, temperature and LAI, respectively

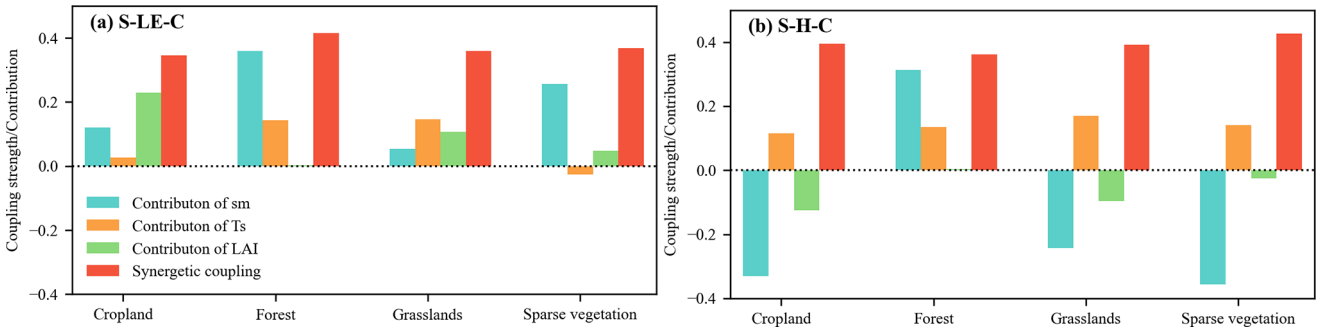

Fig. 13 Surface synergetic coupling and contribution of surface factors in different ecosystems, (**a**) for synergetic coupling of LE and (**b**) for synergetic coupling of H

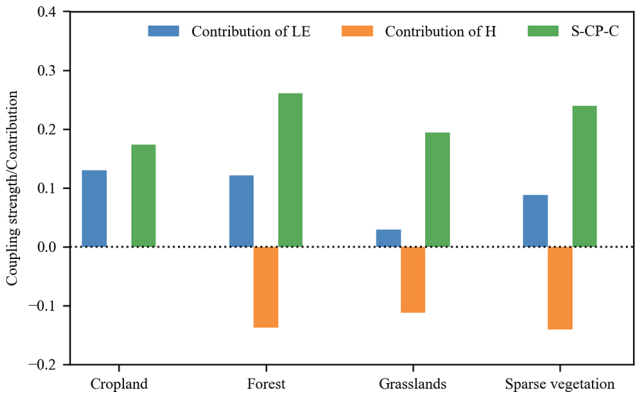

Fig. 14 Atmospheric synergistic coupling (S-P-C) and contribution of H and LE in different ecosystems

contribution in cropland, grasslands, and sparse vegetation areas, while its contribution in forests is weak. In summary, LE is primarily controlled by LAI in cropland, dominated by soil moisture in forests and sparse vegetation areas, and influenced by surface temperature in grasslands; H is primarily controlled by soil moisture across all types of vegetation types.

Figure 14 shows differences in atmospheric synergetic coupling strength and contributions of surface flux among to precipitation under different land surface cover types. S-CP-C is larger in forested and sparsely vegetated areas compared to cropland and grassland areas. Specifically, LE contributes more to CP in cropland and forests, followed by sparse vegetation, and is less significant in grasslands; H exhibits a relatively large negative contribution in forests, grasslands, and sparse vegetation areas, with almost no contribution in land. Therefore, afternoon convective precipitation is primarily driven by latent heat in cropland, influenced by both sensible and latent heat in forest, and mainly controlled by sensible heat in grasslands and sparse vegetation areas.

5 Discussions

The results of this study show that the contribution of surface temperature to sensible heat (H) is relatively small, while soil moisture has a larger contribution. This seems counterintuitive since surface temperature generally has a direct impact on H and its contribution is expected to be large. In fact, the influence of surface temperature on H is generally more pronounced on daily or sub-daily scales (Ma and Ma 2016). At the monthly scale considered in this study, on the eastern slope of the Tibetan Plateau, the relative variability of soil moisture is significantly larger than that of soil temperature (Fig. 2b, d), with the relative variability of soil moisture being approximately four times larger than that of soil temperature. The much smaller variability in soil temperature leads to a smaller contribution to sensible heat.

This study explores the impact of land surface conditions on precipitation, finding that 16% of precipitation variability can be explained by sensible heat and latent heat (LE). When focusing solely on afternoon precipitation variability, H and LE can account for up to 36% of the precipitation changes. The study only takes into account the linear effects of surface factors on precipitation, while there are also nonlinear effects (Hsu and Dirmeyer 2021). This likely underestimates the contribution of H and LE to precipitation. Nevertheless, the dominant contributions to precipitation are complex atmospheric dynamics and environmental conditions(Wang et al. 2018), such as moisture convergence and uplift, atmospheric stability, which are closely related to atmospheric circulation (Lai et al. 2024). Additionally, in the rugged terrain of the eastern slope of the Tibetan Plateau, complex topography is also an important factor affecting precipitation (Imamovic et al. 2017).

The sensitivity of coupling strength to surface moisture and ecological factors, along with the significant differences among various ecosystems, highlights the substantial impact of surface heterogeneity on land-atmosphere coupling. The influence of temporal and spatial variations in surface moisture conditions on coupling strength has been

broadly acknowledged (Guillod et al. 2015; Wei and Dirmeyer 2012). The role of vegetation physiological and ecological processes in land-atmosphere coupling has received less attention. Changes in vegetation conditions can shift the soil moisture-evapotranspiration coupling from positive to negative through stomatal regulation mechanisms (Williams and Torn 2015). Increased vegetation cover can reduce albedo, increase net radiation, and heat the atmosphere, causing the planetary boundary layer height to exceed the lifting condensation level, resulting in more convective clouds (Manoli et al. 2016). It can also lower surface temperatures through increased transpiration, thus reducing atmospheric heating. Additionally, differences in vegetation roughness can lead to variations in turbulence intensity, thereby affecting the formation of deep convection (Chen et al. 2020). Therefore, the relative importance of these processes varies among different vegetation types, leading to notable differences in land-atmosphere coupling across different vegetation conditions (Tao et al. 2019).

This study dissected the coupling between multiple land surface variables and precipitation across the northeastern slope of the Tibetan Plateau. Some aspects might contribute to the uncertainty of the results. First, the complex topography of the study region would induce mountain-valley circulation and trigger precipitation(Barton et al. 2021). Large scale dynamics also produce precipitation (Welty and Zeng 2018). Since large-scale precipitation often persists and results in morning rainfall, excluding days with morning precipitation helps reduce the uncertainty related to large-scale precipitation (Taylor et al. 2012). Therefore, this study using afternoon precipitation could reduce these impacts. Second, although sensible and latent heat flux data in this study are widely used, they still have considerable uncertainties over the complex surface of the northeastern slope of the plateau. Finally, coupling were only characterized statistically, and exploring the specific coupling mechanisms requires more detailed boundary layer 3-D observations and numerical experiments.

6 Conclusions

To elucidate the influence of changes in land surface state on precipitation across the northern slope of the Tibetan Plateau, this study investigates the spatial distribution of land-atmosphere coupling and its influencing factors. Based on an understanding of the spatiotemporal distribution of land surface states, surface fluxes, and precipitation, this study characterizes the spatial distribution of land-atmosphere coupling through a two-step coupling analysis, considering land surface state-surface flux coupling and surface flux-precipitation coupling. Synergetic coupling strength significantly are enhanced compared to individual couplings. During the surface coupling stage, the synergetic coupling strength is strongest in the northwestern desert region and increases southeastward for latent heat flux, is more complicated for sensible heat flux. During the atmospheric coupling stage, latent heat flux positively influences afternoon precipitation, particularly in the northwest, whereas sensible heat flux generally has a negative impact. The synergetic coupling is further enhanced when considering precipitation components (convection and large-scale precipitation).

Moreover, this study examines the variations in coupling strength with land surface state factors. Land surface coupling is sensitive to the variation of climatology of surface factors. For the surface coupling stage, the coupling strength of surface variables with latent heat flux increases first and then decreases with increasing soil moisture, and that with sensible heat flux weakens with increasing soil moisture. With increasing LAI, the synergetic coupling of surface variables with latent heat gradually increases, and that with sensible heat gradually decreases. For the atmospheric coupling stage, the synergetic coupling decreases first and then increases with increasing soil moisture, strengthens with increasing surface temperature, and weakens with increasing LAI.

Finally, it compares the coupling strength and contributions of various factors across different land cover types. Land-atmosphere coupling and factor contributions vary in different ecosystems. For the surface coupling stage, the synergetic coupling of surface variables with latent heat is larger in forested areas than in other areas, while that with sensible heat is largest in sparse vegetation areas, followed by croplands and grasslands, and smallest in forests. Latent heat is dominated by soil moisture in forests and sparse vegetation, and by LAI in croplands, and by surface temperature in grasslands. Sensible heat is dominated by soil moisture in all land surface types. For the atmospheric coupling stage, the synergetic coupling is relatively strong in forests and sparse vegetation areas, and weak in croplands and grasslands. Afternoon precipitation is mainly dominated by latent heat in cropland, jointly influenced by sensible and latent heat in forest, and mainly dominated by sensible heat in grassland and sparse vegetation.

Acknowledgements This work was jointly supported by National Natural Science Foundation of China (U2142208) and (42230610), and the Second Tibetan Plateau Scientific Expedition and Research (STEP) program (grant no. 2019QZKK0102).

Author contributions ZY and PY conceived the study. ZY, HH, HY, and QZ performed the analyses and wrote the initial draft of the manuscript. All authors contributed to the interpretation of the results, discussion of the associated mechanisms, and refnement of the paper.

Data availability No datasets were generated or analysed during the

current study.

Declarations

Competing interests The authors declare no competing interests.

References

Barton EJ, Taylor CM, Klein C, Harris PP, Meng X (2021) Observed soil moisture impact on strong convection over mountainous tibetan Plateau. J Hydrometeorol 22:561–572. https://doi.org/10.1175/JHM-D-20-0129.1

Betts AK, Ball JH, Beljaars ACM, Miller MJ, Viterbo PA (1996) The land surface-atmosphere interaction: a review based on observational and global modeling perspectives. J Geophys Res: Atmos 101:7209–7225. https://doi.org/10.1029/95JD02135

Chen J, Hagos S, Xiao H, Fast JD, Feng Z (2020) Characterization of Surface Heterogeneity-Induced Convection using cluster analysis. J Geophys Res: Atmos 125:e2020JD032550 https://doi.org/10.1029/2020JD032550.

Dirmeyer PA, Wang Z, Mbuh MJ, Norton HE (2014) Intensified land surface control on boundary layer growth in a changing climate. Geophys Res Lett 41:1290–1294. https://doi.org/10.1002/2013gl058826

Entin JK, Robock A, Vinnikov KY, Hollinger SE, Liu S, Namkhai A (2000) Temporal and spatial scales of observed soil moisture variations in the extratropics. J Geophys Res: Atmos 105:11865–11877. https://doi.org/10.1029/2000JD900051

Fan K, Zhang Q, Singh VP, Sun P, Song C, Zhu X, Yu H, Shen Z (2019) Spatiotemporal impact of soil moisture on air temperature across the Tibet Plateau. Sci Total Environ 649:1338–1348. https://doi.org/10.1016/j.scitotenv.2018.08.399

Findell KL, Eltahir EAB (1997) An analysis of the soil moisture-rainfall feedback, based on direct observations from Illinois. Water Resour Res 33:725–735. https://doi.org/10.1029/96WR03756

Gao C, Chen H, Sun S, Xu B, Ongoma V, Zhu S, Ma H, Li X (2018) Regional features and seasonality of land–atmosphere Coupling over Eastern China. Adv Atmos Sci 35:689–701. https://doi.org/10.1007/s00376-017-7140-0

Gerken T, Ruddell BL, Yu R, Stoy PC, Drewry DT (2019) Robust observations of land-to-atmosphere feedbacks using the information flows of FLUXNET. npj Clim Atmos Sci 2:37. https://doi.org/10.1038/s41612-019-0094-4

Guillod BP, Orlowsky B, Miralles DG, Teuling AJ, Seneviratne SI (2015) Reconciling spatial and temporal soil moisture effects on afternoon rainfall. Nat Commun 6:6443. https://doi.org/10.1038/ncomms7443

Haghighi E, Short Gianotti DJ, Akbar R, Salvucci GD, Entekhabi D (2018) Soil and Atmospheric controls on the Land Surface Energy Balance: a generalized Framework for distinguishing Moisture-Limited and Energy-Limited evaporation regimes. Water Resour Res 54:1831–1851. https://doi.org/10.1002/2017WR021729

Hobeichi S, Abramowitz G, Evans J, Ukkola A (2018) Derived optimal Linear Combination Evapotranspiration (DOLCE): a global gridded synthesis ET estimate. Hydrology Earth Syst Sci (Online) 22. https://doi.org/10.5194/hess-22-1317-2018

Hsu H, Dirmeyer PA (2021) Nonlinearity and multivariate dependencies in the Terrestrial Leg of Land-Atmosphere Coupling. Water Resour Res 57:e2020WR028179 https://doi.org/10.1029/2020WR028179.

Hu H, Leung LR, Feng Z (2021) Early warm-season mesoscale convective systems dominate soil moisture–precipitation feedback for summer rainfall in central United States. Proceedings of the National Academy of Sciences 118:e2105260118. https://doi.org/10.1073/pnas.2105260118

Huang J, Zhou X, Wu G, Xu X, Zhao Q, Liu Y, Duan A, Xie Y, Ma Y, Zhao P, Yang S, Yang K, Yang H, Bian J, Fu Y, Ge J, Liu Y, Wu Q, Yu H, Wang B, Bao Q, Qie K (2023) Global climate impacts of Land-Surface and Atmospheric processes over the Tibetan Plateau. Rev Geophys 61:e2022RG000771 https://doi.org/10.1029/2022RG000771.

Imamovic A, Schlemmer L, Schär C (2017) Collective impacts of Orography and Soil moisture on the Soil moisture-precipitation feedback. Geophys Res Lett 44:11,682–611,691. https://doi.org/10.1002/2017GL075657

Koster RD (2004) Regions of strong coupling between soil moisture and precipitation. Science 305:1138–1140. https://doi.org/10.1126/science.1100217

Koster RD, Suarez MJ, Liu P, Jambor U, Berg A, Kistler M, Reichle R, Rodell M, Famiglietti J (2004) Realistic initialization of Land Surface States: impacts on Subseasonal Forecast Skill. J Hydrometeorol 5:1049–1063. https://doi.org/10.1175/jhm-387.1

Lai H-W, Chen D, Chen HW (2024) Precipitation variability related to atmospheric circulation patterns over the Tibetan Plateau. Int J Climatol 44:91–107. https://doi.org/10.1002/joc.8317

Li M, Ma Z, Gu H, Yang Q, Zheng Z (2017) Production of a combined land surface data set and its use to assess land-atmosphere coupling in China. J Geophys Res: Atmos 122:948–965. https://doi.org/10.1002/2016jd025511

Ma W, Ma Y (2016) Modeling the influence of land surface flux on the regional climate of the Tibetan Plateau. Theor Appl Climatol 125:45–52. https://doi.org/10.1007/s00704-015-1495-x

Ma Y, Hu Z, Xie Q, Meng X, Zhao L, Dong W (2022) Convection-permitting modeling over the Tibetan Plateau improves the simulation of Meiyu Rainfall during the 2011 Yangtze Plain flood. Atmos Res 265:105907. https://doi.org/10.1016/j.atmosres.2021.105907

Ma Y, Yao T, Zhong L, Wang B, Xu X, Hu Z, Ma W, Sun F, Han C, Li M, Chen X, Wang J, Li Y, Gu L, Xie Z, Liu L, Sun G, Wang S, Zhou D, Zuo H, Xu C, Liu X, Wang Y, Wang Z (2023) Comprehensive study of energy and water exchange over the Tibetan Plateau: a review and perspective: from GAME/Tibet and CAMP/Tibet to TORP, TPEORP, and TPEITORP. Earth Sci Rev 237:104312. https://doi.org/10.1016/j.earscirev.2023.104312

Manoli G, Domec J-C, Novick K, Oishi AC, Noormets A, Marani M, Katul G (2016) Soil–plant–atmosphere conditions regulating convective cloud formation above southeastern US pine plantations. Global Change Biol 22:2238–2254. https://doi.org/10.1111/gcb.13221

Meng L, Shen Y (2014) On the relationship of Soil Moisture and Extreme temperatures in East China. Earth Interact 18:1–20. https://doi.org/10.1175/2013ei000551.1

Meng X, Li R, Luan L, Lyu S, Zhang T, Ao Y, Han B, Zhao L, Ma Y (2018) Detecting hydrological consistency between soil moisture and precipitation and changes of soil moisture in summer over the Tibetan Plateau. Clim Dyn 51:4157–4168. https://doi.org/10.1007/s00382-017-3646-5

Meng X, Mao K, Meng F, Shi J, Zeng J, Shen X, Cui Y, Jiang L, Guo Z (2021) A fine-resolution soil moisture dataset for China in 2002–2018. Earth Syst Sci Data 13:3239–3261. https://doi.org/10.5194/essd-13-3239-2021

Petrova IY, van Heerwaarden CC, Hohenegger C, Guichard F (2018) Regional co-variability of spatial and temporal soil moisture–precipitation coupling in North Africa: an observational perspective. Hydrol Earth Syst Sci 22:3275–3294. https://doi.org/10.5194/hess-22-3275-2018

Rodell M, Houser PR, Jambor U, Gottschalck J, Mitchell K, Meng CJ, Arsenault K, Cosgrove B, Radakovich J, Bosilovich M, Entin JK, Walker JP, Lohmann D, Toll D (2004) The Global Land Data

Assimilation System. Bull Am Meteorol Soc 85:381–394. https://doi.org/10.1175/bams-85-3-381
Ruscica RC, Sörensson AA, Menéndez CG (2015) Pathways between soil moisture and precipitation in southeastern South America. Atmos Sci Lett 16:267–272. https://doi.org/10.1002/asl2.552
Santanello JA, Dirmeyer PA, Ferguson CR, Findell KL, Tawfik AB, Berg A, Ek M, Gentine P, Guillod BP, van Heerwaarden C, Roundy J, Wulfmeyer V (2018) Land–atmosphere interactions: the LoCo Perspective. Bull Am Meteorol Soc 99:1253–1272. https://doi.org/10.1175/bams-d-17-0001.1
Seneviratne SI, Lüthi D, Litschi M, Schär C (2006) Land–atmosphere coupling and climate change in Europe. Nature 443:205–209. https://doi.org/10.1038/nature05095
Sulla-Menashe D, Gray JM, Abercrombie SP, Friedl MA (2019) Hierarchical mapping of annual global land cover 2001 to present: the MODIS Collection 6 Land Cover product. Remote Sens Environ 222:183–194. https://doi.org/10.1016/j.rse.2018.12.013
Sun G, Hu Z, Ma Y, Xie Z, Sun F, Wang J, Yang S (2021) Analysis of local land atmosphere coupling characteristics over Tibetan Plateau in the dry and rainy seasons using observational data and ERA5. Sci Total Environ 774:145138. https://doi.org/10.1016/j.scitotenv.2021.145138
Talib J, MÜLler OV, Barton EJ, Taylor CM, Vidale PL (2023) The representation of Soil moisture–atmosphere feedbacks across the Tibetan Plateau in CMIP6. Adv Atmos Sci 40:2063–2081. https://doi.org/10.1007/s00376-023-2296-2
Talib J, Taylor CM, Duan A, Turner AG (2021) Intraseasonal Soil moisture–atmosphere feedbacks on the tibetan Plateau circulation. J Clim 34:1789–1807. https://doi.org/10.1175/JCLI-D-20-0377.1
Tang Q, Xie S, Zhang Y, Phillips TJ, Santanello JA, Cook DR, Riihimaki LD, Gaustad KL (2018) Heterogeneity in Warm-Season Land-Atmosphere Coupling over the U.S. Southern Great Plains. J Geophys Res: Atmos 123:7867–7882. https://doi.org/10.1029/2018JD028463
Tao C, Zhang Y, Tang S, Tang Q, Ma H-Y, Xie S, Zhang M (2019) Regional Moisture Budget and Land-Atmosphere Coupling over the U.S. Southern Great Plains inferred from the ARM Long-Term observations. J Geophys Res: Atmos 124:10091–10108. https://doi.org/10.1029/2019JD030585
Taylor CM, de Jeu RA, Guichard F, Harris PP, Dorigo WA (2012) Afternoon rain more likely over drier soils. Nature 489:423–426. https://doi.org/10.1038/nature11377
Wan Z (2014) New refinements and validation of the collection-6 MODIS land-surface temperature/emissivity product. Remote Sens Environ 140:36–45. https://doi.org/10.1016/j.rse.2013.08.027
Wang X, Pang G, Yang M (2018) Precipitation over the Tibetan Plateau during recent decades: a review based on observations and simulations. Int J Climatol 38:1116–1131. https://doi.org/10.1002/joc.5246
Wei J, Dirmeyer PA (2012) Dissecting soil moisture-precipitation coupling. Geophys Res Lett. https://doi.org/10.1029/2012gl053038. 39:n/a-n/a
Welty J, Zeng X (2018) Does Soil Moisture Affect Warm Season Precipitation Over the Southern Great Plains? Geophys Res Lett 45:7866-7873. https://doi.org/10.1029/2018GL078598
Wenze Y, Bin T, Dong H, Rautiainen M, Shabanov NV, Wang Y, Privette JL, Huemmrich KF, Fensholt R, Sandholt I, Weiss M, Ahl DE, Gower ST, Nemani RR, Knyazikhin Y, Myneni RB (2006) MODIS leaf area index products: from validation to algorithm improvement. IEEE Trans Geosci Remote Sens 44:1885–1898. https://doi.org/10.1109/TGRS.2006.871215
Williams IN, Torn MS (2015) Vegetation controls on surface heat flux partitioning, and land-atmosphere coupling. Geophys Res Lett 42:9416–9424. https://doi.org/10.1002/2015gl066305
Yang K, He J (2019) In: Plateau Data C (ed) China meteorological forcing dataset (1979–2018). National Tibetan Plateau Data Center, National Tibetan
Yang K, Wang C (2022) East–West Reverse Coupling between Spring Soil moisture and summer precipitation and its possible responsibility for Wet Bias in GCMs over Tibetan Plateau. J Geophys Res: Atmos 127:e2021JD036286 https://doi.org/10.1029/2021JD036286.
Zeng X, Barlage M, Castro C, Fling K (2010) Comparison of land–precipitation coupling strength using observations and models. J Hydrometeorol 11:979–994. https://doi.org/10.1175/2010jhm1226.1
Zeng Y, Xie Z (2015) Projection and evaluation of the land-atmosphere coupling strength over China by CMIP5 models. Clim Environ Res 20:337–246
Zhao P, Xu X, Chen F, Guo X, Zheng X, Liu L, Hong Y, Li Y, La Z, Peng H, Zhong L, Ma Y, Tang S, Liu Y, Liu H, Li Y, Zhang Q, Hu Z, Sun J, Zhang S, Dong L, Zhang H, Zhao Y, Yan X, Xiao A, Wan W, Liu Y, Chen J, Liu G, Zhaxi Y, Zhou X (2018) The Third Atmospheric Scientific experiment for understanding the earth–atmosphere coupled system over the Tibetan Plateau and its effects. Bull Am Meteorol Soc 99:757–776. https://doi.org/10.1175/bams-d-16-0050.1
Zscheischler J, Orth R, Seneviratne SI (2015) A submonthly database for detecting changes in vegetation-atmosphere coupling. Geophys Res Lett 42:9816–9824. https://doi.org/10.1002/2015gl066563